Light Metals 2014

ELECTRODE TECHNOLOGY FOR ALUMINUM PRODUCTION

Inert Anodes, Cathode Design and Alternative Processes

SESSION CHAIR

Gregory Goupil

Institut National de la
Recherche Scientifique (INRS)
Varennes, QC, Canada

EFFECT OF LA ON THE ELECTROLYSIS PERFORMANCE OF
46Cu-25Ni-19Fe-10Al METAL ANODE

Peng Weiping, Liu Ying, Guo Jie, Zhao Ruilong, Yang Jianhong, Li Wangxing

Zhengzhou Research Institute of Chalco, Zhengzhou, Henan 450041, China

Abstract

With addition of La element for modification of 46Cu-25Ni-19Fe-10Al metal anode material, the 200A/815℃ electrolytic test showed that the precipitation of La element at the grain boundary hindered the outward migration of metal atoms and the inward diffusion of oxygen atoms. Meanwhile, a compact composite oxide scale (including Cu_2O, NiO, $CuFe_2O_4$ and $NiFe_2O_4$.) is formed on the surface of the anode during the test. Due to the pinning effect of La elements, the oxide scale was closely combined with the metal matrix and impeded the electrolyte penetration, thereby reducing anodic corrosion rate and dissolution of the oxide scale. This alloy has a potential to be an inert anode in industrial aluminum electrolysis.

Introduction

In recent years, among the possible inert anode materials (metal/alloys, cermets and ceramics), metal anodes appear to be most interesting in the international research [1-4], because of their high strength, good electrical conductivity, excellent thermal shock resistance, and mechanical property, ease of manufacture and simplicity for electrical connection to the current metal rod. The major challenge for metal anodes is to obtain a material having an excellent high temperature corrosion resistance under aluminum electrolysis conditions. Namely, it requires to forming a uniform, compact, relatively thin and protective scale with self-healing ability at the surface of the anode. Recently, Cu-based alloys are focused on in some metal inert anode research [5-10]. During aluminum electrolysis, Cu-based alloys generate composite oxide scale at the surface. The oxide scale can protect the metal matrix and cause less voltage drop. Meanwhile impurity in produced aluminum could be controlled to an extent by suppressing dissolution of the oxide scale.

In this paper, the rare earth La element is added to improve the uniformity and compactness of the oxide scale and the adhesion between the oxide scale and metal matrix. Thus, dissolution of the oxides is reduced and the metal matrix is effectively protected.

Experimental

An alloy identified as A062 alloy (nominal composition w.t.%: 46Cu-25Ni-19Fe-10Al) was selected as a promising inert anode material through a number of high temperature oxidation tests and 20A electrolysis tests. The alloy has good resistance to high temperature oxidation and excellent corrosion resistance to electrolyte. However, for improving its scale formation, A063 alloy was obtained by adding 1.0% La into the A062 alloy by vacuum induction melting.

The 200A electrolysis experiments were done in $NaF-KF-AlF_3$-Al_2O_3 electrolyte inside a graphite crucible, with cryolite ratio between 1.25 and 1.45, alumina concentration between 5.0% and 7.0%, between 800℃ and 830℃. Anodic current density was 0.6A/cm^2 and anode-cathode-distance was 3 cm. After the electrolysis, the samples were analyzed by SEM and EDX.

Results and discussion

200A electrolysis test

The 200A electrolysis test results indicate that the A062 and A063 alloys both have good electrolysis properties. The voltage curves are shown in Fig.1. The voltage fluctuation of the A062 alloy is larger, between 3.7V and 4.1V, while the voltage of the A063 alloy is relatively stable, between 3.6V and 3.9V. Also, the scale of the A063 alloy after electrolysis is uniform and smooth, and the shape of the anode retains more its integrity. The optical digital photos of the A062 and A063 alloys after electrolysis are shown in Fig.2, which manifests the rare earth elements can greatly improve the electrolysis performance of the metal anode. The microstructure of the matrix, the inner oxide scale on the metal surface and the outer spalling scale of the anode after electrolysis would be compared in the following passages. The structure of the two scales and the mechanism of the scale formation will be discussed.
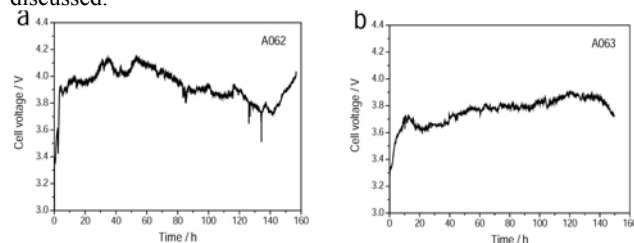

Figure 1. The electrolysis voltage curves: (a) A062 and (b) A063
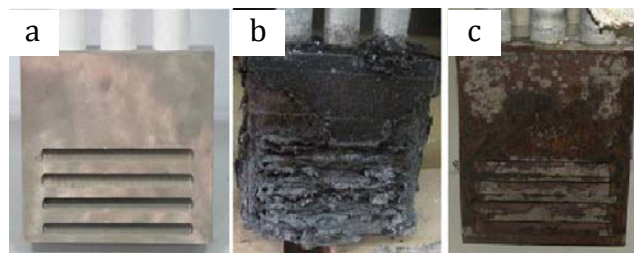

Figure 2. The morphology of the alloys before and after test: (a) pre-experiment (b) A062 alloy and (c) A063 alloy

Microstructure of the metal matrix

The SEM images of the A062 and A063 alloys are shown in Fig.3. It can be found that microstructure of the A062 alloy consists of Cu-rich α phase with little Al and β-NiAl phase, which is acicular-like with 30-50μm length and 5-10μm width. The

effect of Al was to improve oxidation-resistance and reduce thickness of the scale. The Al content in the α-phase is too low to form protective scale Al_2O_3. But on the whole, the microstructure of A062 alloy is uniform with the second dispersed phase, β-NiAl. The Cu-rich α-phase in A063 alloy has more Al content than A062 alloy. The β-NiAl phase are spherical with radius 25-100μm. The white third phase, mainly distributed at grain boundary is Cu_6La. The enrichment of rare earth La at boundary limits diffusion and migration of metal atoms such as Al, Fe, Ni, Cu, which influences the scale formation process and mechanism.
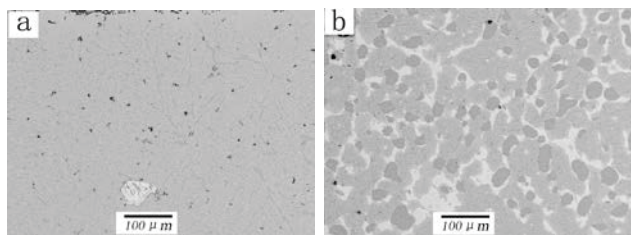

Figure 3. Microstructure of the alloys: (a) A062 and (b) A063

Structure of the inner oxide scale

The cross-sectional morphologies of the inner layer oxide scales after electrolysis are shown in Fig.4. It can be found that the inner layer scale of the A062 alloy is thin, with the thickness of 100μm. The external 30μm thick part of the scale is a mixture of oxides and electrolyte. The middle part is an oxide/metal interface, with thickness of 30μm. The internal layer of the scale is Cu-rich metal matrix, with no NiAl detected. Meanwhile, the film is not uniform, continuous and cohesive. On the contrary, the electrolytic scale of the A063 alloy is a relatively thicker, approximately 200μm in thickness. The external part of the film is 50μm thickness, composed of anode element-constitutive oxides. At the oxide/metal interface, NiAl phase is found. All of the differences listed above undergo different scale formation mechanisms to form protective oxide on the anodes surface.
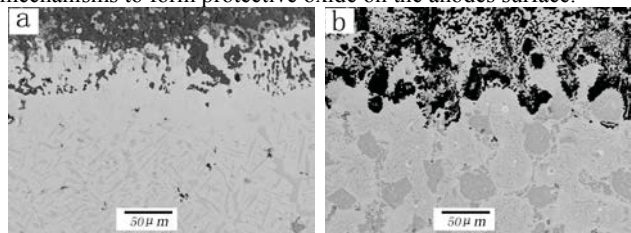

Figure 4. The cross-sectional of inner oxides scale of the alloys: (a) A062 and (b) A063

Fig.5 shows XRD analysis of the oxide scales of the two alloys. We noticed only a lot amount of Cu_2O and NiO oxides in the A062 scale. This scale partly contains electrolyte and fluoride, which means the surface oxide scale of the A062 alloy is not protective and cannot prohibits electrolyte penetration. On the contrary, the scale of the A063 alloy is composed of binary oxides and spinel oxides, including Cu_2O, NiO, $CuFe_2O_4$ and $NiFe_2O_4$. A small amount of electrolyte is observed at the alloy-oxide interface, indicating that the scales are protective. However, it needs to be improved because of the bad uniformity and continuity of the scale.
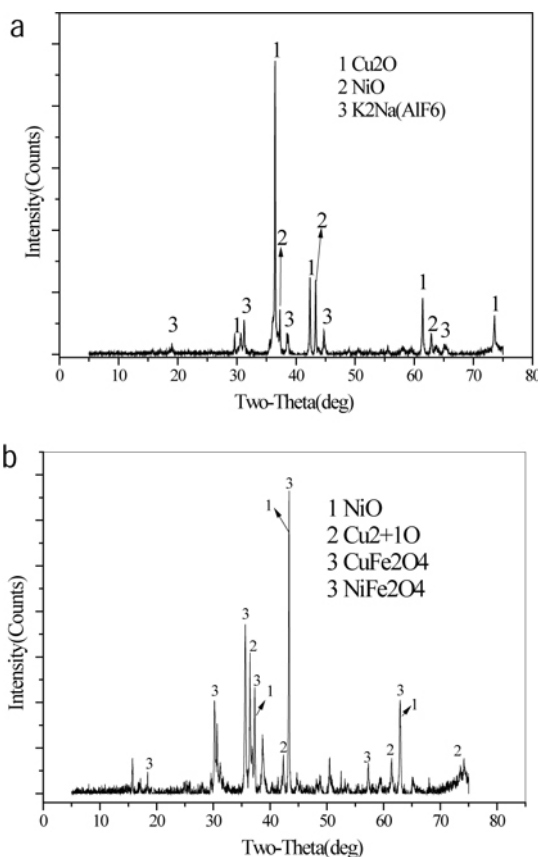

Figure 5. The XRD analysis of the oxides: (a) A062 and (b) A063

The components of the oxide/metal interface and internal metal matrix of A062 and A063 are shown in Fig. 6. A Cu-rich zone can be found at the outer part of the alloy A062, and no Al could be found. Near the alloy bulk, Al content reached 6%, but decreased to zero on the scale/metal interface. The phenomenon indicated that the exterior Al atoms migrated to the surface and were oxidized to Al_2O_3 which was prefer to dissolution, but the inner Al atoms had slow migration rate in the metal matrix and were gradually deplete in the near-scale areas. As a result, the oxide scale became unstable and discontinuous. Nevertheless, the oxide/metal interface for A062 alloy was mainly composed of a Cu-rich layer. The Cu_2O and NiO scale was totally no protective leading to a more severe A062 alloy corrosion. For A063 alloy, observed phases at the interface area and the matrix are similar. The Al content of the interface area is 4%, and a large amount of Ni-Al phase could be found, which indicates there was no Al depleted zone. The grain boundaries are usually high speed migration channels for metal atoms (Al, Fe, Cu) and oxygen atoms diffusion. However, the large La atoms segregated at the grain boundary could block the channels and slow down the migration speed. The Ni-Al phase presented at the interface area of A063 alloy was oxidized to Cu_2O, NiO, $CuFe_2O_4$ and $NiFe_2O_4$. These oxides formed a dense scale to hinder electrolyte penetration. So A063 seems more corrosion-resistant than A062.
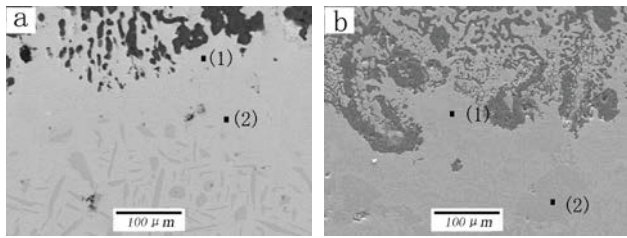
(1): 90Cu-9Ni-1Fe   (1): 49Ni-34Cu-13Fe-4Al
(2): 53Cu-25Ni-16Fe-6Al   (2): 36Ni-35Cu-15Fe-14Al

Figure 6. Chemical components of the matrix:
(a) A062 and (b) A063

The EDS element maps for the cross-section of A063 alloy after electrolysis were shown in Fig. 7. The high content of Fe in all of the scale, scale/Metal interface and matrix (Fig.7 Fe) means the components of the scale include $NiFe_2O_4$ and $CuFe_2O_4$, which also can be seen from the Fig.5(b). The "net-like structure" of La map (Fig.7 La) proved the "pinning effect". The light area of the map represents La oxide. Since LaO is easy to form, the LaO gathers at the grain boundary and reaches deeply into the metal matrix, adheres the oxide scale to the metal matrix just like a "pin". Furthermore, the large radii of La atoms, makes metal elements hard to diffuse, which have enhanced the "pinning effect" [11].
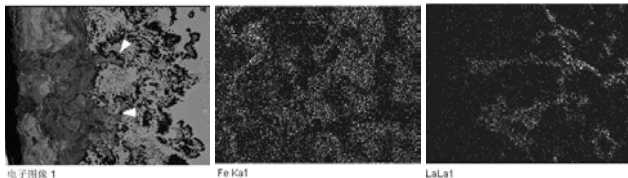

Figure 7. The EDS element maps for the cross-section of A063 alloy after electrolysis

Structure of the outer oxide scale

Fig. 8 is the SEM cross-section images of the spalling oxide scales formed after electrolysis of the (a) A062 and (b) A063. The spalling scale of A062 is loose and has the almost 2000μm thickness. In this scale, the element strength of Cu is stronger than that of Ni and Fe, that is to say the main component of the scale is Cu_2O or CuO. In the A063 outer scale, the element strength of Ni and Fe is both stronger than Cu, which indicates that the oxidation of Ni and Fe such as $CuFe_2O_4$ and $NiFe_2O_4$ constitute the A063 outer scale. This scale is dense and 1000μm thick protects the alloy more effectively from electrochemical corrosion.
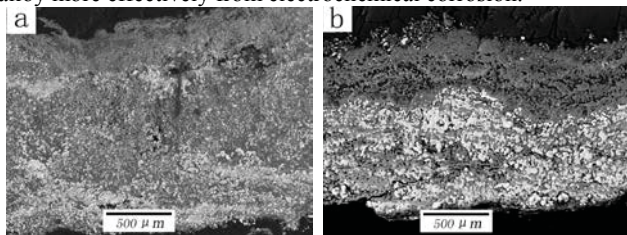

Figure 8. SEM cross-section images of the outer oxide scales:
(a) A062 and (b) A063

Fig. 9 is the schematic of composition of the scales formed after electrolysis on the (a) A062 and (b) A063. Based on the analysis above, for A062, as the Al, Fe, Ni atoms migrating rapidly outside the scale, the oxide scale was mainly composed of Cu_2O and NiO,

this scale was loosen and porous, could not protect the alloy very effectively from penetration of the electrolyte. For A063, the gathering of La atoms at grain boundaries have blocked the path of the Al, Fe, Ni atoms migration, the oxide scale was composed of Cu_2O, NiO, $CuFe_2O_4$ and $NiFe_2O_4$, this dense and corrosion resistant scale, protects the alloy more effectively from penetration of the electrolyte.
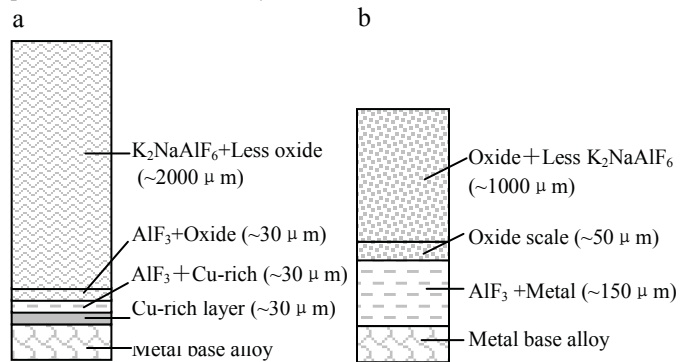

Figure 9. The schematic of composition of the oxide scales:
(a) A062 and (b) A063

Conclusions

1. With high speed migration of Al, Fe, Ni atoms, a Cu-rich layer has been formed at the near scale/matrix interface area in A062. The Cu_2O and NiO scale was loose and porous, could not protect the alloy very effectively from electrochemical corrosion.

2. La atoms gathering at grain boundary of A063 alloy blocked the outward diffusion channels of metal elements. During the electrolysis, the metal elements reacted with O atoms at the scale/matrix interface area, and formed oxide scale including Cu_2O, NiO, $CuFe_2O_4$ and $NiFe_2O_4$. This dense scale could protect the alloy from penetration of electrolyte. The A063 alloy has a potential to be an inert anode in industrial aluminum electrolysis.

3. The "pinning effect" of La element connected the oxide scale to the metal matrix, enhanced the adhesive strength of the scale, and reducing the anodic corrosion and dissolution rate of the A063 alloy oxide scale..

References

1. Barry J. Welch, "Inert anodes- the status of the materials science, the opportunities they present and the challenges that need resolving before commercial implementation", *Light metals*, TMS, 2009: 971-978.

2. Vittorio de Nora, "Thinh Nguyen. Inert anode: Challenges from fundamental research to industrial application", *Light metals*, TMS, 2009: 417-421.

3. Jianhong Yang, John Hryn et al, "New opportunities for aluminum electrolysis with metal anodes in a low temperature electrolyte system", *Light Metals*, TMS, Warrendale, PA. 2004: 321-326.

4. He Hanbing, Li Zhiyou, and Zhou Kechao, "Research Progress in Metal Inert Anodes", *Materials Review*, 2007, 21(12): 69-72.

5. Haugsrud D R, and Kofstad P, "On the high-temperature oxidation of Cu-rich Cu-Ni alloys", *Oxidation of Metals*, 1998, 50(3/4):189-213.

6.   Reidar Haugsud, "On the influence of non-protective CuO on high-temperature oxidation of Cu-Ni based alloys", *Oxidation of Metals*, 1999, 53(5-6):427-445.

7.   Reidar Haugsrud, Truls Norby, and Per Kofstad, "High-temperature oxidation of Cu-30 wt.% Ni-15 wt.% Fe", *Corrosion Science*, 2001, 43: 283-299.

8.   Mark Glucina, and Margaret Hyland, "Laboratory-scal performance of a binary Cu-Al alloy as an anode for aluminum electrowinning", *Corrosion Science*, 2006, (48):2457-2469.

9.   Badr Assouli, et al., "Mechanically alloyed Cu-Ni-Fe based materials as inert anode for aluminum production", *Light metals*, TMS, 2009:1141-1144.

10.   Qiu Zhuxian, Xu Junli, and Shi Zhongning, "New inert anode in aluminum electrolysis", *The Chinese Journal of Nonferrous Metals*，2004, 14(1): 36-41.

11.   A.S.Khanna, *Introduction to high temperature oxidation and corrosion*, (Replike Press, India, 2002), 220-223.